mathematics

MDPI

Article

Stochastic Final Pit Limits: An Efficient Frontier Analysis under Geological Uncertainty in the Open-Pit Mining Industry

Enrique Jelvez [1,*], Nelson Morales [2] and Julian M. Ortiz [3]

[1] Advanced Mining Technology Center, Delphos Mine Planning Laboratory & Department of Mining Engineering, University of Chile, Santiago 8370451, Chile
[2] Civil, Geology and Mining Engineering Department, Polytechnique Montréal, Montreal, QC H3T 1J4, Canada; nelson.morales@polymtl.ca
[3] The Robert M. Buchan Department of Mining, Queen's University, Kingston, ON K7L 3N6, Canada; julian.ortiz@queensu.ca
* Correspondence: enrique.jelvez@amtc.uchile.cl

Abstract: In the context of planning the exploitation of an open-pit mine, the final pit limit problem consists of finding the volume to be extracted so that it maximizes the total profit of exploitation subject to overall slope angles to keep pit walls stable. To address this problem, the ore deposit is discretized as a block model, and efficient algorithms are used to find the optimal final pit. However, this methodology assumes a deterministic scenario, i.e., it does not consider that information, such as ore grades, is subject to several sources of uncertainty. This paper presents a model based on stochastic programming, seeking a balance between conflicting objectives: on the one hand, it maximizes the expected value of the open-pit mining business and simultaneously minimizes the risk of losses, measured as conditional value at risk, associated with the uncertainty in the estimation of the mineral content found in the deposit, which is characterized by a set of conditional simulations. This allows generating a set of optimal solutions in the expected return vs. risk space, forming the Pareto front or efficient frontier of final pit alternatives under geological uncertainty. In addition, some criteria are proposed that can be used by the decision maker of the mining company to choose which final pit best fits the return/risk trade off according to its objectives. This methodology was applied on a real case study, making a comparison with other proposals in the literature. The results show that our proposal better manages the relationship in controlling the risk of suffering economic losses without renouncing high expected profit.

Keywords: stochastic final pit; geostatistics; open-pit mining; risk management; Pareto-optimal front

Citation: Jelvez, E.; Morales, N.; Ortiz, J.M. Stochastic Final Pit Limits: An Efficient Frontier Analysis under Geological Uncertainty in the Open-Pit Mining Industry. *Mathematics* **2022**, *10*, 100. https://doi.org/10.3390/math10010100

Academic Editors: Víctor Yepes and José Moreno-Jiménez

Received: 22 November 2021
Accepted: 22 December 2021
Published: 28 December 2021

1. Introduction

In simple terms, the final pit limit problem is defined as determining the ultimate mining limits of an ore deposit exploited by the open-pit mining method such that a maximum undiscounted profit is obtained from its extraction, respecting the precedence constraints given by overall slope angles that ensure stable walls of the open-pit mine.

The final pit limit plays a crucial role in long-term open-pit mine production planning. It approximates the placement, size, shape, and depth of the mine at the end of its exploitation, determining important aspects for mine operation such as the layout of access roads, ramps, waste dumps, stockpiles, processing, and other facilities, as well as in developing a production schedule. Besides, different studies such as feasibility analyses, assessment of capital exposure, and corporate risk can be considerably affected by the results of non-optimum final pit limit determination [1].

As a first step, the ore deposit is modelled as a regular array of blocks, known as the block model. This model is constructed by interpolating information available at drill hole samples obtained from the terrain. Several attributes are estimated, such as rock types, concentrations (grades) of relevant elements, and density, among others, using

geostatistical estimation techniques [2]. Then, an economic value that represents its profit is computed for each block. This value depends on the estimated geological attributes and economic and operational parameters such as ore price, costs, and metallurgical recoveries. The result of this is called the economic block model and is the primary input for pit limit optimization [3].

The final pit decision is contemplated in the initial stages of strategic open-pit mine planning and can be solved efficiently by using Lerchs—Grossmann [4] or Pseudoflow [5,6] algorithms. However, as indicated before, it is based on a single, smooth representation of the deposit [7]; therefore, the in-situ geological uncertainty is not taken into account. This type of uncertainty comes from an incomplete knowledge of the ore deposit considering a reduced number of drill hole samples, restricted by exploration costs, limiting the estimation accuracy of the geological attributes. According to [8], the quality of the estimation depends mainly on the following: (i) the placement, quantity, and quality of the samples, (ii) the orebody classification, and (iii) the method used to generate the estimations.

As mine exploitation progresses, new sample information is generated, and the block model is updated. However, strategic mine planning decisions (such as mining sequence) have already been made, causing deviations in the planned production promises. As a result of the traditional approach, mining companies are often incapable of fulfilling production promises due to their inability to evaluate and minimize the consequences of geological uncertainty in the early stages of a mining project [9–12].

Conditional simulation is a geostatistical method for modelling geological uncertainty and a valuable tool for risk assessment in pit designs, generating equally probable scenarios (realizations) that represent the in-situ orebody variability [13–15]. There are many approaches for conditional simulation of continuous random variables, such as ore grades as used in this work. Some are based on a normal score transformation and the assumption of multi-Gaussianity. These include sequential Gaussian simulation [2,16,17], turning bands simulation [18] and matrix decomposition simulation [19]. Other methods rely on an approximation of the conditional distribution done by defining thresholds and creating indicator variables, which are characterized through sequential indicator simulation [20]. In recent years, more advanced methods that use multiple-point statistics have been developed [21,22] to simulate, accounting for patterns. Simulated annealing [23], direct sequential simulation [24], and p-field simulation [25] provide other approaches that do not require the same assumptions of the abovementioned methods.

Assuming there is a set of scenarios characterizing the geological uncertainty, for instance rock type and ore grades, the first challenge in mine planning is how to use this information to assess its impact on the plan. One option could be to obtain one final pit per scenario separately, and from them, decide of a single final pit, based on some well-defined criteria (Figure 1). A completely different option is a model that does not consider the input data (set of scenarios) separately but can consider them simultaneously in one run and thus compute a single robust optimal final pit (Figure 2).

However, because the final pit is one of the most critical and higher impact decisions in a mining project, some questions arise:

- What final pit should be chosen for a given confidence level in terms of economic value or metal content from all possible options? or,
- How would the final pit contour change if the ore grade variability is higher or lower than expected?

Unfortunately, the traditional methodology to compute final pit limits cannot give answers to these critical questions. For this reason, it is crucial to generate robust final pit methodologies that consider geological uncertainty, especially at the beginning of a mining project, when a high level of uncertainty is present.

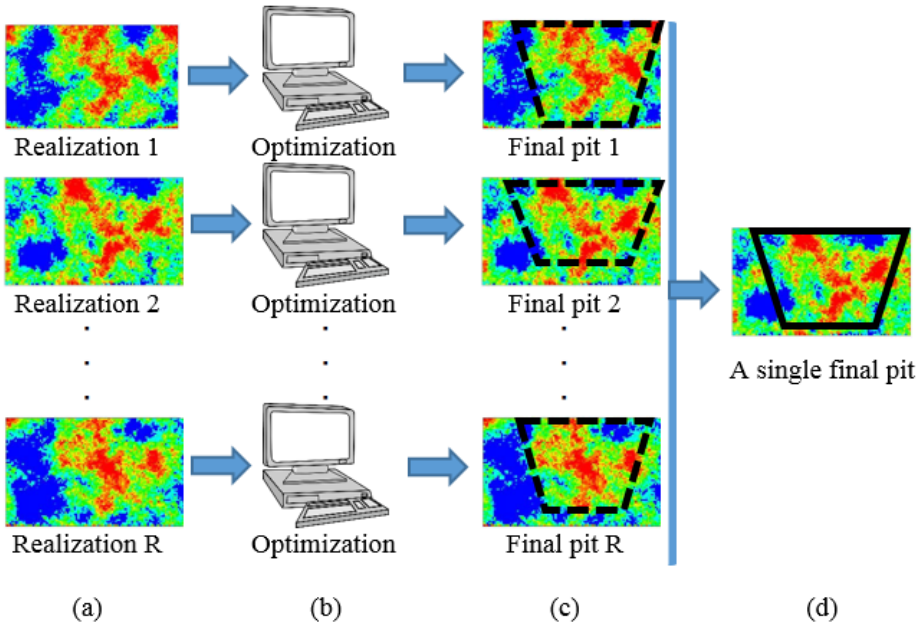

Figure 1. A first approach to compute final pit limit: (**a**) a set of realizations representing the geological uncertainty are used as input individually, (**b**) the optimization computes a final pit for each realization, (**c**) a set of partial solutions are given, and (**d**) applying some criteria, a single final pit limit is selected.

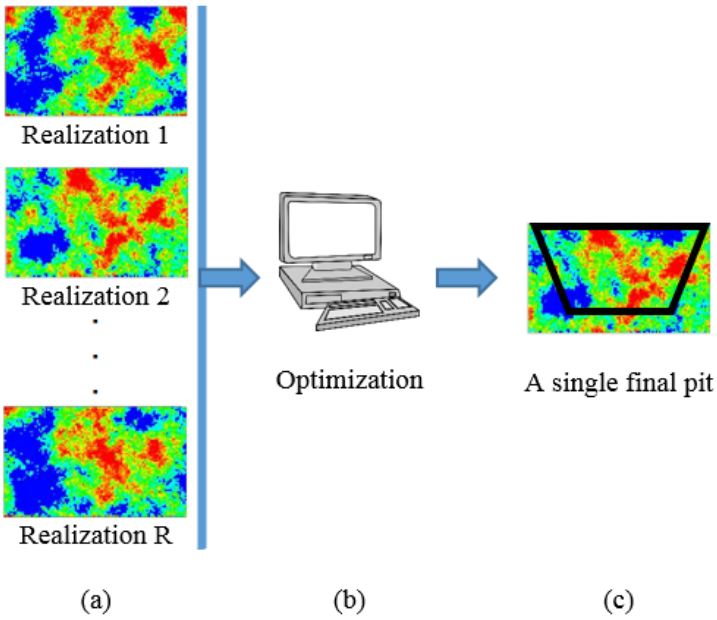

Figure 2. A second approach to compute final pit limit: (**a**) a set of realizations representing the geological uncertainty are used as input simultaneously, (**b**) the optimization computes a single solution for the entire set of realizations, and (**c**) a robust final pit limit is returned.

One of the first efforts to include geological uncertainty into the final pit limit is by [26], which presented a hybrid approach within a set-theory framework. This work considered final pits for several simulated realizations of the orebody and then defined the so-called hybrid pit. Later, Refs. [10,27,28] compute pits based on the hybrid approach and propose some reliability indexes for a pit. Ref. [29] proposed to use one of the simulated pits as the best pit design, capturing the upside potential of the orebody and minimizing the potential downside risk. Ref. [30] presented a workflow that includes the computation of a series of

nested pits, considering the simulations of the block model and distributions of economic and geotechnical parameters as inputs.

The above approaches can be used as a guide to assess the risk associated with geological uncertainty; however, their main drawback is that the optimization process does not incorporate risk control. The solution is only obtained after a series of final pit limit problems are solved separately, following the approach presented in Figure 1.

On the other hand, under the approach showed in Figure 2, we can identify the following contributions: Ref. [31] presented the advantages of using a stochastic approach based on expected economic values rather than expected ore grades, from a set of simulated realizations of ore grade. Ref. [32] proposed a constrained version of the problem, incorporating the risk management directly into the optimization model in a probabilistic framework. In the same line, refs. [33,34] incorporated grade uncertainty on a modified version of the model for the final pit limit problem, where extraction and processing decisions are taken separately, proposing a two-stage scheme. Ref. [35] used risk measures to incorporate geology and market uncertainty into the investment, pit design, and mining sequence decisions, but unfortunately, they do not perform the methodology on a real case study.

More recently, Ref. [36] develops a mean-variance criterion approach to finding near-optimal final pit limits by using a heuristic procedure considering geological uncertainty, generating a set of solutions on the mean-variance efficient frontier. Then, based on some stochastic dominance rules, the authors eliminate sub-optimal solutions. Some drawbacks of this approach are (i) standard deviation as a risk measure does not consider skewness and (ii) the proposed heuristic algorithm cannot guarantee an optimal solution because it uses a greedy optimizer, and, besides, some parameters of the algorithm must be chosen manually. A second work, ref. [37], focuses on the theoretical problem and proposes properties that a risk-averse measure for final pit limit should have (i) nestedness of pits for different risk aversion levels and (ii) additive consistency, which states that extraction order should not be affected by the precedence of farther parts of the mine. They show that only an entropic risk measure complies with these properties and propose an approximation scheme based on a two-stage stochastic model. Finally, interesting research was developed by [38], who presented a comprehensive overview of the applications and trends of multi-criteria decision-making methods applied in mining and mineral processing problems.

In this paper, we propose a methodology based on a stochastic optimization model that maximizes expected profit while controlling maximum risk in terms of conditional value at risk in mining projects and apply it to a real case study. The orebody is modelled through several simulated realizations to incorporate explicit risk control in open-pit mine design and evaluation. As a result, the efficient frontier of final pit limit alternatives in the expected profit vs. risk environment is obtained. Additionally, we propose some criteria to choose pits from the efficient frontier depending on the decision maker's risk aversion.

2. Materials and Methods: Modelling, Notation, and Problem Statement

In this section, we present the main notation and formulation for the final pit limit problem. Section 2.1 presents the model for the deterministic case of the final pit, and Section 2.2 introduces basic concepts of conditional value at risk. Based on these preliminary concepts, Section 2.3 states the problem addressed in this work by providing a formulation to compute the final pit considering a representation of geological uncertainty explicitly.

2.1. Final Pit Limit: Deterministic Case

Let B be the block model and b a block. $PREC_b \subset B - \{b\}$ denotes the subset of blocks above block b that must be extracted before it, respecting maximum slope angles.

An economic block value $\overline{v}_b$ is precomputed for block b. By using integer programming, the decision variables are defined as

$$x_b = \begin{cases} 1, & \text{if block } b \text{ belongs to the final pit,} \\ 0, & \text{otherwise} \end{cases} \tag{1}$$

Thus, the final pit limit is the solution to the following

$$(P)\ max \quad \sum_{b \in B} \overline{v}_b\, x_b \tag{2}$$

$$s.t. \quad x_b \leq x_a \qquad \forall b \in B,\ a \in PREC_b \tag{3}$$

$$x_b \in \{0,1\} \qquad \forall b \in B \tag{4}$$

where Equation (2) represents the maximum undiscounted total profit of blocks within final pit limits. Equation (3) ensures that the shape of the ultimate pit respects the overall slope angle, and Equation (4) indicates the decision variables are binary. There exist fast algorithms to solve this problem [5,6,39]. As stated above, the geological uncertainty is not considered in this formulation. Therefore, this model does not capture the risk associated with a non-accurate ore resource estimation.

2.2. Background on Risk Measures: Conditional Value at Risk

In mining under geological uncertainty, the term *risk* refers to the potential economic losses caused by a misleading ore resource estimation. One tool used to reduce the risk of losses is the value at risk (VaR). Let $\delta \in (0,1)$ be the risk level and $f(\boldsymbol{x},\boldsymbol{y})$ a loss function for a decision vector $\boldsymbol{x} \in X$ and a random vector $\boldsymbol{y} \in \mathbb{R}^m$. For a given $\boldsymbol{x}$, $f(\boldsymbol{x},\boldsymbol{y})$ is a random variable having a distribution into $\mathbb{R}$ induced by $\boldsymbol{y}$. $\Psi(\boldsymbol{x},\zeta)$ is the probability that the loss function $f(\boldsymbol{x},\boldsymbol{y})$ does not exceed a threshold value ζ, that is, $\Psi(\boldsymbol{x},\zeta) = \mathbb{P}[f(\boldsymbol{x},\boldsymbol{y}) \leq \zeta]$. $\Psi(\boldsymbol{x},\zeta)$ is the cumulative distribution for the loss associated to $\boldsymbol{x}$, which depends on ζ considering $\boldsymbol{x}$ as fixed. Thus,

$$\mathrm{VaR}_\delta(\boldsymbol{x}) = \min\{\zeta \in \mathbb{R} :\ \Psi(\boldsymbol{x},\zeta) \geq \zeta\} \tag{5}$$

However, this risk measure has some drawbacks, as reported in [40], such as lack of sub-additivity or lack of control by losses exceeding VaR. Thus, Rockafellar and Uryasev [41] propose a different measure of risk, namely the conditional value at risk (CVaR), which represents the conditional expected loss given that the loss exceeds VaR. For continuous distributions

$$\mathrm{CVaR}_\delta(\boldsymbol{x}) = (1-\delta)^{-1} \int_{f(\boldsymbol{x},\boldsymbol{y}) > VaR_\delta(\boldsymbol{x})} f(\boldsymbol{x},\boldsymbol{y})\ p(\boldsymbol{y})\ d\boldsymbol{y} \tag{6}$$

where $p(\boldsymbol{y})$ is the density of $\boldsymbol{y}$. To avert difficulties with $\mathrm{VaR}_\delta(\boldsymbol{x})$ into Equation (6), Rockafellar and Uryasev give an alternative representation that characterizes both $\mathrm{VaR}_\delta(\boldsymbol{x})$ and $\mathrm{CVaR}_\delta(\mathrm{x})$ in terms of F_δ on $X \times R$:

$$\mathrm{F}_\delta(\boldsymbol{x},\zeta) = \zeta + (1-\delta)^{-1} \int_{\boldsymbol{y} \in \mathbb{R}^m} (f(\boldsymbol{x},\boldsymbol{y}) - \zeta)\ p(\boldsymbol{y})\ d\boldsymbol{y} \tag{7}$$

quantifying the losses that exceed VaR, acting as an upper bound for it at the same confidence level δ. Besides, CVaR is convex and a coherent risk measure [42], allowing the implementation of optimization algorithms to determine it. The integral in Equation (7) can be approximated in several ways: for instance, by sampling the probability distribution

of $\boldsymbol{y}$ according to its density $p(\boldsymbol{y})$ from which a collection of R equally probable vectors $\boldsymbol{y}^1, \ldots, \boldsymbol{y}^R$ is obtained. Therefore, the corresponding approximation to $F_\delta(\boldsymbol{x}, \zeta)$ is

$$\widetilde{\mathrm{F}}_\delta(\boldsymbol{x}, \zeta) = \zeta + \frac{1}{R\,(1-\delta)} \sum_{r=1}^{R} [f(\boldsymbol{x}, \boldsymbol{y}^r) - \zeta]^+ \tag{8}$$

where $[t]^+ = \max\{t, 0\}$. As shown in [41], an approximation of minimum CVaR is found by minimizing Equation (8). Note that the optimization simultaneously gives the optimal decision $\boldsymbol{x}^*$, $\mathrm{VaR}_\delta(\boldsymbol{x}^*)$, and $\mathrm{CVaR}_\delta(\boldsymbol{x}^*)$. Henceforth, when we refer to CVaR, we strictly mean the approximation to CVaR, since geological uncertainty is represented employing a finite number of scenarios. Finally, to avoid the non-linear function $[f(\boldsymbol{x}, \boldsymbol{y}^r) - \zeta]^+$ into Equation (8), we will use auxiliary variables z_r, for all $r \in \mathcal{R} = \{1, \ldots, R\}$,

$$[f(\boldsymbol{x}, \boldsymbol{y}^r) - \zeta]^+ = \{z_r \geq 0 \,:\, z_r \geq f(\boldsymbol{x}, \boldsymbol{y}^r) - \zeta\} \tag{9}$$

Further details on minimization of CVaR can be found in [41]; for properties and strong and weak features of the VaR and CVaR risk measures, see [42]; and for illustrations with several examples, see [43]. Applications on optimization problems, including CVaR constraints, are addressed in [44].

2.3. Problem Statement: Risk-Based Final Pit Limit

Consider several realizations $\boldsymbol{y}^1, \ldots, \boldsymbol{y}^R$ of random variable $\boldsymbol{y}$ from resource models indexed by $r \in \mathcal{R}$ to represent the geological uncertainty. For example, $\boldsymbol{y}^r$ may be interpreted as the ore grade or metal content according to realization r. In this case,

$$\boldsymbol{y}^r = (y_{br})_{b \in B} \qquad \forall\, r \in \mathcal{R} \tag{10}$$

An economic block model can be stated per realization, i.e., v_{br} indicates the block value according to the metal content y_{br} from realization $r \in \mathcal{R}$ and block $b \in B$. Contrary to the above, the traditional methodology proposes that a single economic value $\overline{v}_b$ is obtained per block when the metal content $\overline{y}_b$ is estimated by using estimation methods such as inverse distance, kriging, or e-type [2].

As before, the decision vector $\boldsymbol{x} = (x_b)_{b \in B}$ corresponds to the selection of blocks within the final pit limit. Regarding the loss function for each realization $r \in \mathcal{R}$, we propose to measure the losses (or gains) associated with deviations of economic values from each realization regarding an economic value provided according to one of the deterministic/traditional methods. Therefore, the loss function may be expressed as

$$f(\boldsymbol{x}, \boldsymbol{y}^r) = \sum_{b \in B} (\overline{v}_b - v_{br})\, x_b \;\forall\, r \in \mathcal{R} \tag{11}$$

Finally, considering all the above notation, we present the stochastic optimization model that seeks the maximum expected profit under CVaR constraints.

$$(P_\mu)\ max \quad \frac{1}{R} \sum_{b \in B} \sum_{r \in \mathcal{R},} v_{br}\, x_{br} \tag{12}$$

$$s.t. \quad x_b \leq x_a \qquad \forall b \in B,\ a \in PREC_b \tag{13}$$

$$\zeta + \frac{1}{R(1-\delta)} \sum_{r \in \mathcal{R}} z_r \leq \mu \tag{14}$$

$$z_r \geq f(\boldsymbol{x}, \boldsymbol{y}^r) - \zeta \qquad \forall r \in \mathcal{R} \tag{15}$$

$$z_r \geq 0 \qquad \forall r \in \mathcal{R} \tag{16}$$

$$\boldsymbol{x}_b \in \{0, 1\} \qquad \forall b \in B \tag{17}$$

Equation (12) shows the objective function, maximizing expected undiscounted profit of the final pit limit. Equation (13) establishes slope precedence among blocks, and Equation (14) limits the maximum risk $\mu \geq 0$ allowed in terms of CVaR by considering a confidence level $\delta \in (0, 1)$ along R geological scenarios. Equations (15) and (16) are imposed by auxiliary variables, and Equation (17) denotes the nature of decision variables.

Note that an optimal solution (x^*, ζ^*, z^*) to (P_μ) for a given $\mu \geq 0$ determines the blocks inside the final pit limits, the expected undiscounted profit, both VaR (ζ^*) and CVaR, and how the impact of each scenario r into CVaR is distributed.

Varying the parameter value μ in the model (P_μ) allows analysing the trade-off between the (maximum) expected profit of the final pit limit and the (minimum) risk of loss in terms of CVaR. A procedure for defining the set of parameters μ to be considered is as follows:

Procedure 1.

- Find the maximum risk level: to solve the maximum-profit problem, ignoring any constraints on the level of risk, thus obtaining a maximum risk level μ_{max} as CVaR.
- Find the minimum risk level: to solve a minimum-risk problem, ignoring any profit constraint, thus obtaining a minimum risk level μ_{min} as CVaR, and
- Partition the set of possible risk levels: to solve the problem (P_μ) for a set of values

$$\mu = \alpha\ \mu_{min} + (1 - \alpha)\ \mu_{max},\ \alpha \in [0, 1] \tag{18}$$

Figure 3a illustrates the shape of the curve obtained by varying the parameter μ in the expected profit vs. risk plane. Because no final pit above the frontier is possible and alternatives below the frontier are sub-optimal, this curve defines the efficient frontier of final pit alternatives, whether with a higher expected profit keeping the risk bounded or one with lower risk but without reducing profit (see Figure 3b). This boundary allows the investor to make the best decision on which is the final pit of maximum profit, for a given risk level, or to minimize the risk when a particular return is expected.

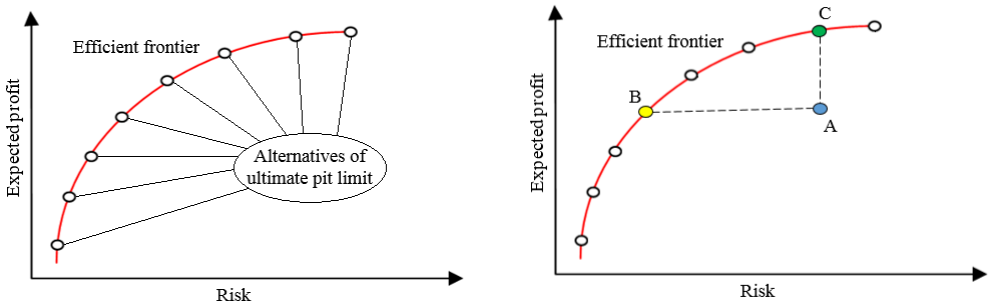

Figure 3. Efficient frontier in the expected profit vs. risk plane. (**a**) Each point represents an alternative to the final pit limit. (**b**) The feasible region under the frontier: point A represents a sub-optimal final pit decision, and points B and C on the efficient frontier are two better alternatives, in terms of risk and expected profit, respectively.

Some of the criteria that a decision maker could use to choose a specific final pit limit from the frontier are the following:

1. (C1) The ideal point is defined as the unfeasible solution located above the frontier, where each criterion is optimized separately (maximum expected return and minimum risk). This criterion proposes to select the final pit that presents the minimum distance to the ideal point. Some distance measures available are Euclidean, normalized, and Manhattan, among others [45].
2. (C2) To select the final pit that reports the most significant difference between expected return and CVaR.
3. (C3) A priori, it is possible that due to the company's internal policies, the decision-maker may not be able to accept projects with a higher risk than a given value μ_0. In this case, the criterion suggests selecting the pit alternative with a higher value and risk limited by μ_0.

4. (C4) Contrary to the previous case, the decision-maker may want to minimize the risk but ensure a minimum return V_0. In this case, the criterion proposes to select the final pit with a minimum CVaR so that the expected return is greater than or equal to V_0.

The interesting results in the efficient frontier are found in the p-range (points of the efficient frontier that are in the p% of a more significant expected profit zone). In general, the final pit limit decision will be taken within this range, looking for the alternative that maintains a high expected profit and reduces the associated risk. Finally, note that it is essential to avoid comparing VaR and CVaR values for the same level of confidence, because they indicate information from different parts of the loss distribution.

3. Implementation and Results

The methods presented in Section 2 are applied to a real porphyry copper deposit as a case study (Section 3.1). The experiments are as follows: (i) generating several optimum final pit alternatives (efficient frontier) for a family of parameters μ (Section 3.2), from a set of simulated realizations, and (ii) comparing in terms os expected profit vs. risk environment, the efficient frontier with the final pit obtained by using the traditional methodology (deterministic case) and other approaches as presented in Figure 1 (Section 4).

To solve the instances of the model (P_μ), GUROBI was used as the optimization solver, version 9.0.3. The code's execution was performed on an Intel Xeon CPU E5-2660 V3 machine with 10 cores at 2.6 GHz, 128 Gb and running Windows 10 Pro.

3.1. Dataset and Instances

The block model corresponds to a porphyry copper deposit (known as BMT, for confidentiality reasons). This block model has 407,179 blocks of 10 m $\times$ 10 m $\times$ 10 m and contains information about spatial coordinates, density, and 50 conditional simulations of copper grade generated by a sequential Gaussian simulation algorithm. In this method, the original samples are transformed to normal scores, and a standard Gaussian random variable is simulated in a spatial grid. Each node of this grid is visited sequentially in a random order, performing a simple kriging estimation using the previously simulated nodes and the normal scores of the true data to condition its value, and drawing a random number from a Gaussian distribution with mean and variance given by the kriging estimate and variance, respectively, to obtain the simulated value, which is then back-transformed to the original grade scale [46]. We assume that the 50 simulated realizations are sufficient to capture the actual variability of copper grades, and we use the E-Type model (average of the 50 realizations) as the standard representation of the metal content estimation considered in the deterministic approach.

Figure 4 shows three different simulated realizations of the copper grade, in addition to the average grade for a plan-view at z = 2015 m.

Figure 5a shows the average histogram of copper grades, including error bars along all sets of realizations. Finally, grade-tonnage curves are plotted to quantify the recoverable resources to different cut-off grades (Figure 5b). Both figures represent error bars with the 5th and 95th percentile per interval, showing low uncertainty in copper grades and ore tonnages.

Precedence arcs and economic block values are provided. In this case, slope precedence requirements respect a 45° overall slope angle in pit walls, but the model can be implemented with other slope angles.

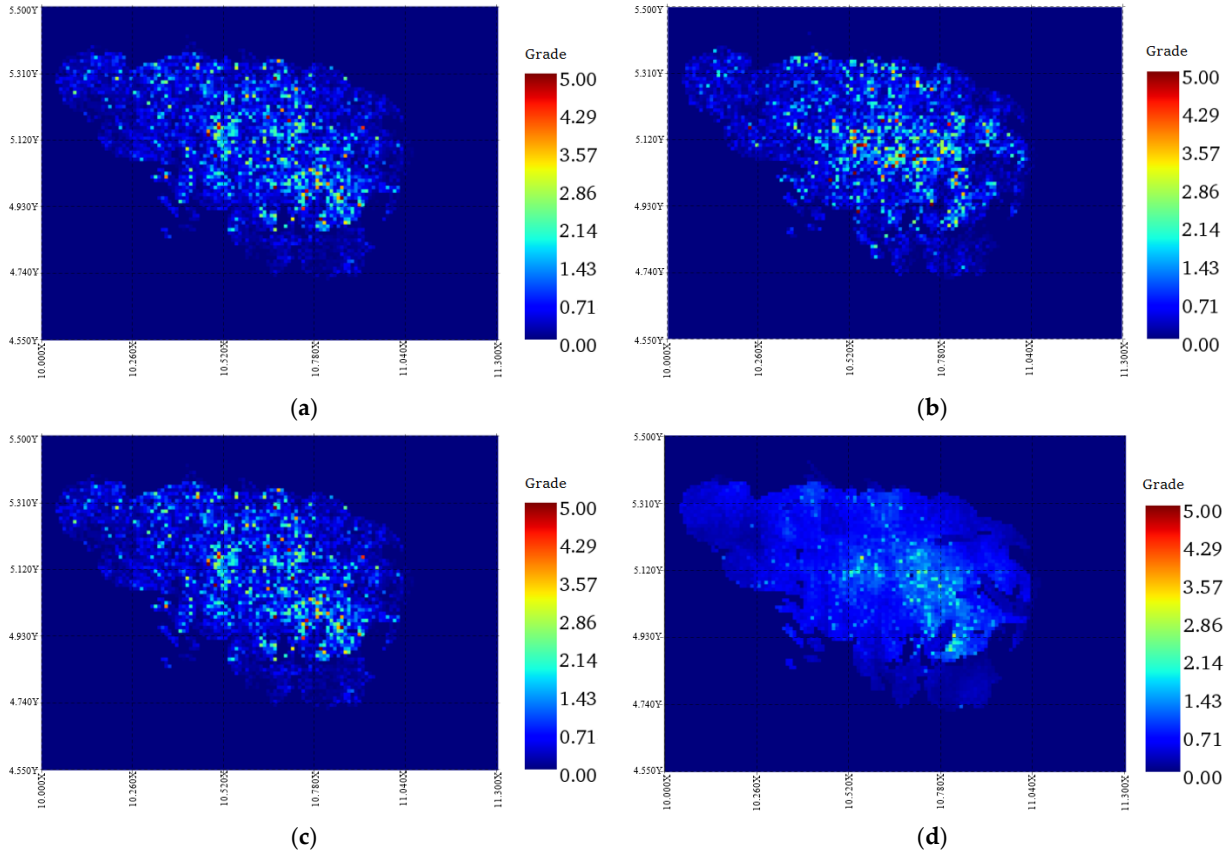

Figure 4. z = 2015 m-plan-views of copper grades for BMT, simulated realizations (**a**–**c**) and E-Type model (**d**).

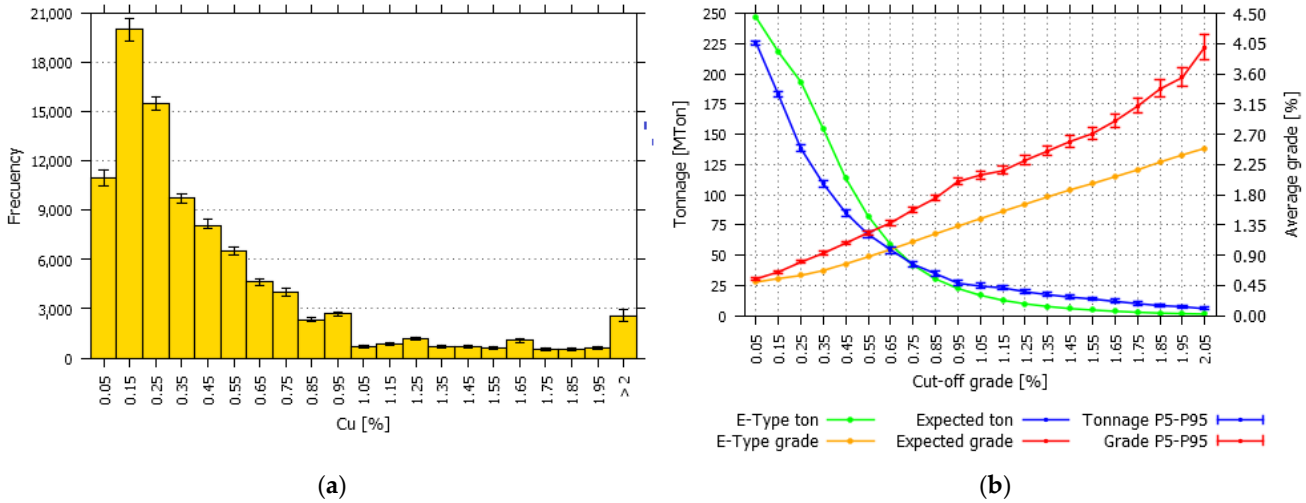

Figure 5. Summary of BMT block model: (**a**) Histogram of copper grades; (**b**) Grade-tonnage curves for the set of simulated realizations and E-Type model. Both graphs include error bars with 5th and 95th percentile per interval.

3.2. Results from Stochastic Model

In this section the results for stochastic final pit limit obtained from model (P_μ) are shown considering a $\delta = 95\%$ confidence level in risk assessment through the CVaR. Applying Procedure 1, Table 1 shows the main numerical results obtained (columns indicate from left to right): the parameter α that determines the maximum risk μ allowed according

to Equation (18), VaR, CVaR, expected profit, and the distance (Euclidean metric) to the ideal point (DIP), which is presented as a decision criterion.

Table 1. Numerical results from efficient frontier for stochastic final pit alternatives obtained with a confidence level of 95%.

α	VaR [MUSD]	CVaR [MUSD]	Exp. Profit [MUSD]	DIP [MUSD]
0.000	155.6	200.0	2058.7	200.0
0.100	155.1	180.0	2053.1	180.1
0.125	151.9	175.0	2049.5	175.2
0.200	139.9	160.0	2035.8	161.6
0.250	139.5	150.0	2022.7	154.3
0.300	132.7	140.0	2009.5	148.4
0.375	123.9	125.0	1982.5	146.4
0.400	120.0	120.0	1970.5	148.9
0.500	96.4	100.0	1904.8	183.5
0.625	73.7	75.0	1727.4	339.6
0.750	49.9	50.0	1551.3	509.8
0.875	24.9	25.0	1016.5	1042.5
1.000	0.0	0.0	0.0	2058.7

All results are within an optimality gap of 1%. Note that the final pit decision yields an empty pit when looking for the minimum risk, i.e., it is equivalent to perform no mining operation. These results allow us to plot the pair (CVaR, expected profit) forming the efficient frontier, or Pareto front (Figure 6a): the points represent different final pit alternatives, each with its respective expected profit and risk. The ideal point (brown) is plotted as a reference according to criterion (C1).

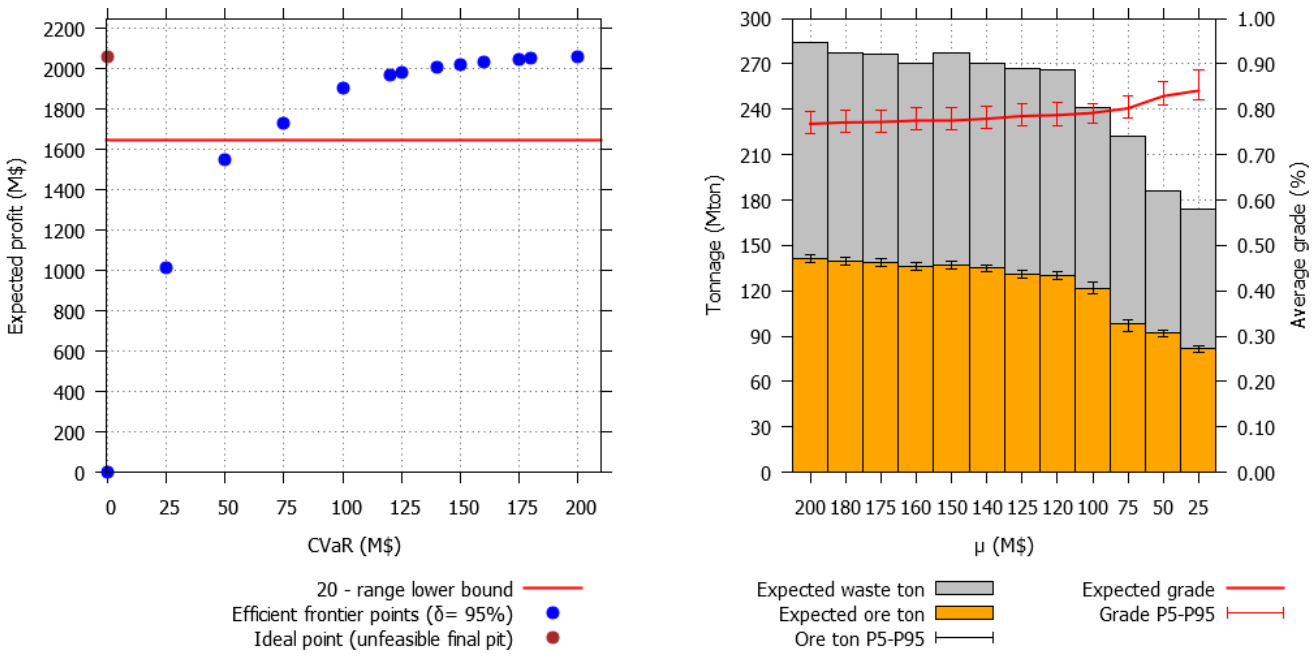

(**a**) (**b**)

Figure 6. Results from efficient frontier applied on BMT block model: (**a**) Efficient frontier between risk (CVaR) and expected profit for the final pit alternatives, with a confidence level of 95%; (**b**) Graph showing ore and waste tonnages and average grade per final pit alternative when varying the parameter μ. Both graphs (ore and grade) include error bars with 5th and 95th percentile per interval.

The interesting results on the efficient frontier are found in the p-range (as explained above). Considering a 20-range, reaching a reduction of up to 20% of expected profit, the final pit alternatives from parameters $\mu = 200$ [MUSD] to $\mu = 75$ [MUSD] are inside this range. The limit case ($\mu = 75$ [MUSD]) includes the final pit whose risk is reduced by approximately 63%, while expected profit drops almost 16%. Regarding the expected tonnages of ore and waste material for each final pit alternative on the efficient frontier, Figure 6 shows how expected ore and waste tonnages decrease as the parameter μ decreases: this should be interpreted as a renunciation of riskier areas within the deposit. Ore tonnage and average grade deviations are represented through error bars showing both the 5th and 95th percentiles along with all geological scenarios.

Figure 7 shows the contribution of z_r to CVaR through $\mathcal{R}$. These contributions are the ones that generate the differences between columns VaR and CVaR in Table 1. Note that the way scenarios contribute to the CVaR is not intuitive because the decision is strongly dependent on the upper bound μ on Equations (14) and (15). In this case study, not all geological scenarios contribute to CVaR in the optimization process; only 11 out of 50 scenarios present total net losses, with realization indexed by $r = 5$ being the one that presents the highest loss. Other scenarios show losses as well, decreasing the total contribution (in MUSD) as the parameter μ decreases, but the final pit with parameter $\mu = 120$ presents VaR = CVaR; therefore, $\sum_{r \in \mathcal{R}} z_r = 0$.

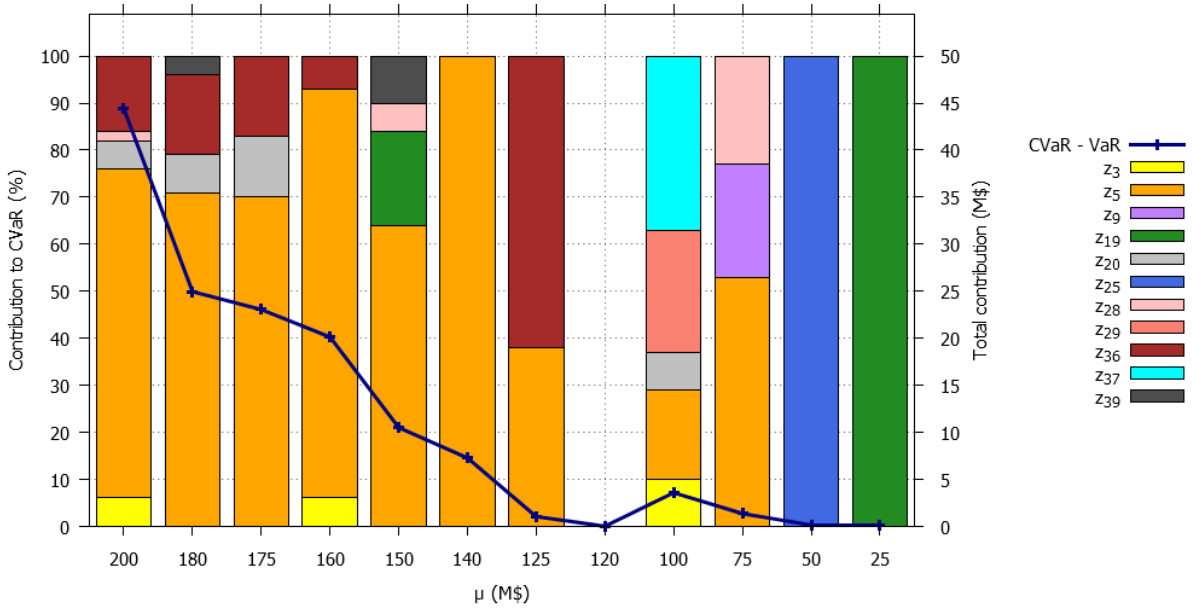

Figure 7. Contribution of z_r to CVaR through $\mathcal{R}$ for each value μ.

Finally, Figure 8 shows plan-views and cross-sections for some final pits, particularly those obtained with parameters $\mu = 200,\ 125,\ 25$. [MUSD]: significant differences in size and shape among the obtained pits can be observed, especially at the bottom of the pits.

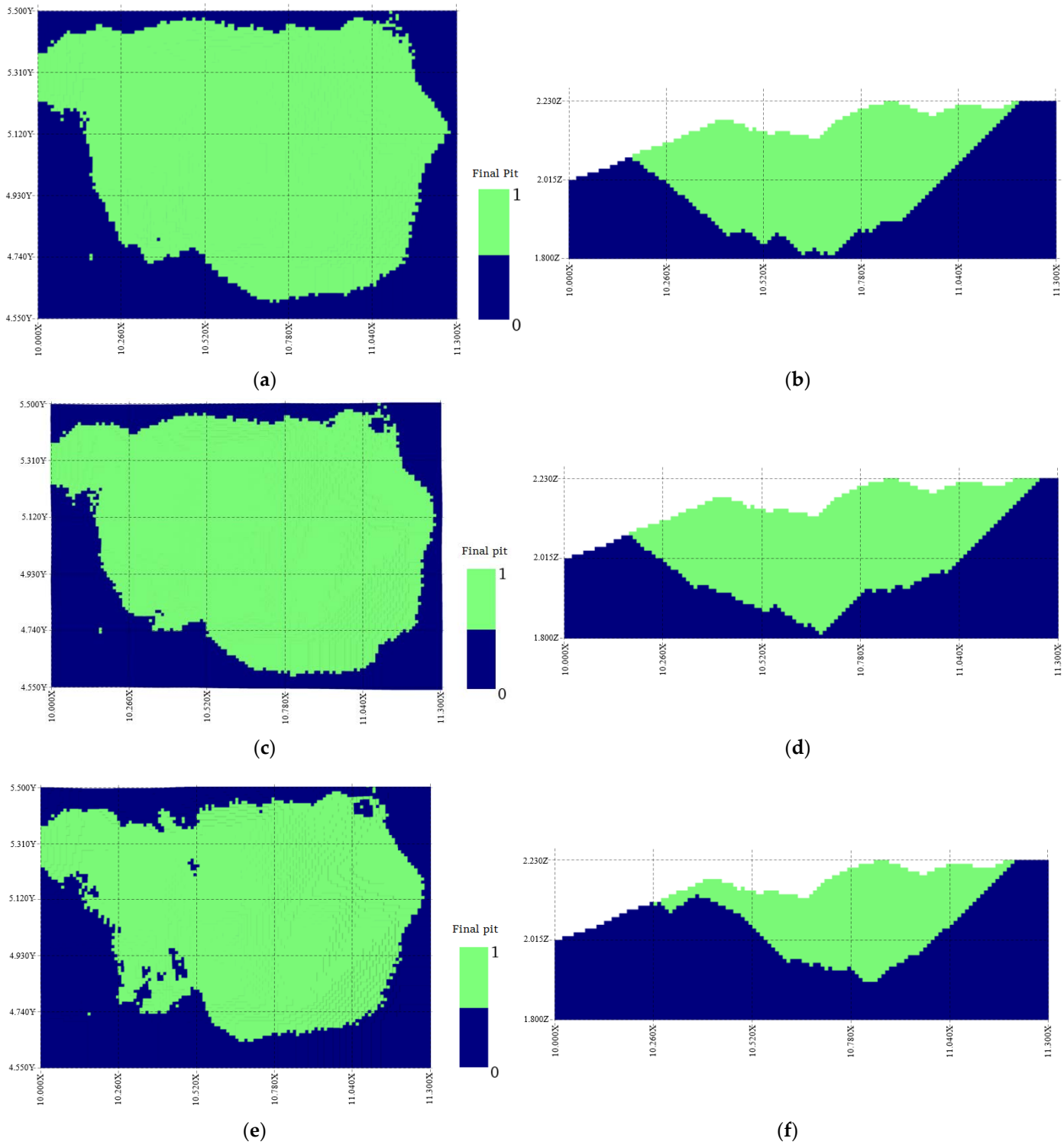

Figure 8. Views of final pit alternatives for the model BMT considering different parameter values $\mu = 200,\ 125,\ 25$ [MUSD] and a confidence level $\delta = 95\%$. (**a**) plan view, final pit $\mu = 200$; (**b**) 5030 m–NS view, final pit $\mu = 200$; (**c**) plan view, final pit $\mu = 125$; (**d**) 5030 m–NS view, final pit $\mu = 125$; (**e**) plan view, final pit $\mu = 25$; (**f**) 5030 m–NS view, final pit $\mu = 25$.

4. Discussion

Once the efficient frontier is determined, it is interesting to know its relative position regarding several final pit decisions obtained from other strategies. In this section we present a comparison of our approach based on the maximization of expected profit but

controlling risk, with other approaches: (i) E-Type, as the only deterministic representation of the deposit; (ii) Expected-profit, as shown in [31]; (iii) Best-simulation as pit design, similar to [29]; and (iv) Hybrid-pit, as presented in [26]. All these results are located in the feasible region within the profit–risk plane. For comparison purposes, the 'best' final pit from the efficient frontier will be chosen according to the criterion (C1) from Section 2.3, that is, by using parameter $\mu = 125$ [MUSD]. However, the same analysis can be generalized by considering other points on the efficient frontier.

In the cases of (i) E-Type, and (ii) Expected-profit, an optimization program (P) defined by Equations (2)–(4) (differentiated by the economic block models) is used to compute a single final pit limit. To find the position of each final pit in the expected profit vs. risk plane, we must solve the program $(P_{\mu_{max}})$ through Equations (12)–(17), but fixing the variables $\boldsymbol{x}_b$ to the values obtained according to the predefined final pit. Therefore, the model $(P_{\mu_{max}})$ only solves for the variable z_r. With this, CVaR and expected profit values can be computed for each final pit. In the cases of (iii) Best-simulation and (iv) Hybrid-pit, 50 different results were obtained, but the chosen ones are those with minimum values according to criterion (C1) after applying model $(P_{\mu_{max}})$.

Figure 9 shows the risk and profit for all methodologies and the reference ideal point. As expected, the final pit from [31] reaches the same result obtained in the efficient frontier with parameter $\mu = 200$ [MUSD]: in this case, the model (P_{μ}) maximizes expected profit regardless of the risk of losses. The rest of the alternatives are suboptimal.

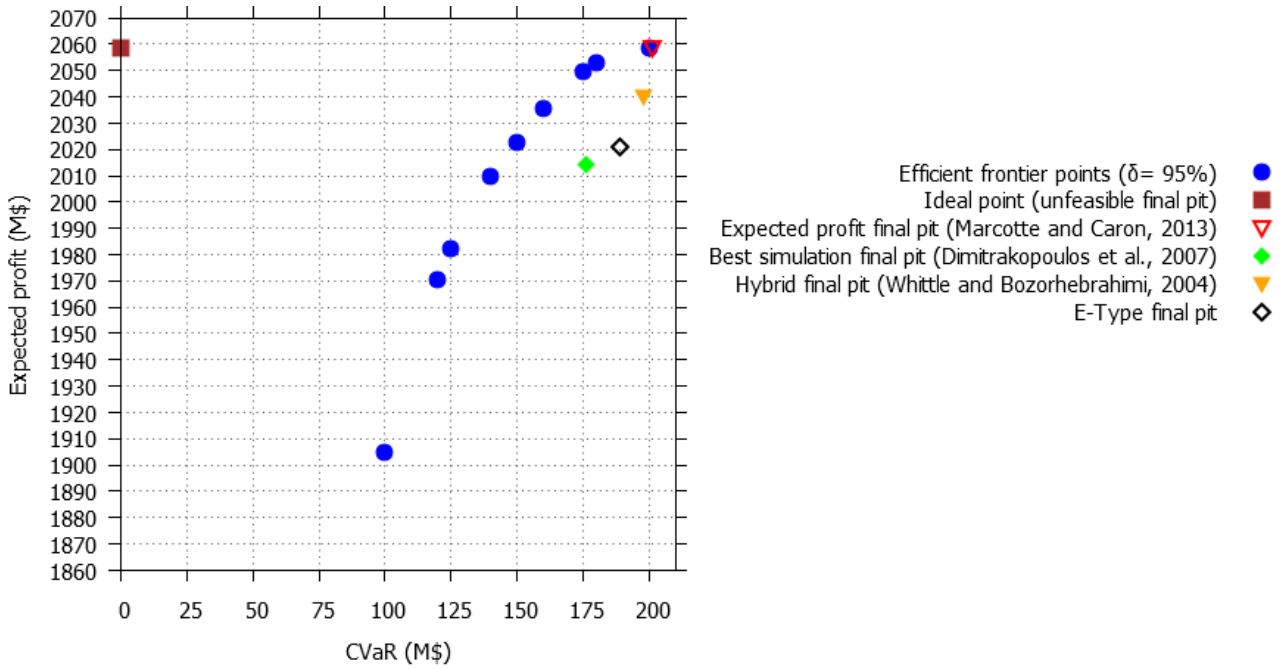

Figure 9. Alternatives of final pits in expected profit vs. risk plane.

Table 2 shows a summary of the comparison: CVaR, expected profit and distance to ideal point (DIP, criterion C1), and their respective relative variations (RV, in %) for each alternative compared to the stochastic final pit obtained with $\mu = 125$ [MUSD], which minimizes DIP, as shown in Table 1. In this case study, there is up to 32% improvement from our stochastic final pit compared to the deterministic one.

Thus, the stochastic final pits in the efficient frontier offer the best trade-off between lower risk in terms of CVaR and higher expected profit when compared to other alternatives, especially the deterministic one. Therefore, applying the proposed model based on stochastic programming reduces the risk and maximizes the expected profit. However, the quantification of this better performance depends on the grade distribution, the representation of geological uncertainty, and the parameters used in each case study. The

efficient frontier's knowledge using geological scenarios allows for making better decisions in strategic open-pit mine production planning regarding expected profit, risk, or both.

Table 2. A comparison among several final pits alternatives in terms of expected profit and risk (CVaR).

Final Pit Method	CVaR [MUSD]	RV%	Exp. Profit [MUSD]	RV%	DIP [MUSD]	RV%
Stochastic (proposed)	125.00	-	1982.50	-	146.37	-
Expected profit	204.28	63.42	2058.65	3.84	204.28	39.56
Best-simulation	176.02	40.81	2013.77	1.58	181.65	24.10
Hybrid-pit	197.64	58.11	2031.07	2.45	199.56	36.34
E-Type	189.34	51.47	2021.45	1.96	192.96	31.83

5. Conclusions and Future Work

This paper develops a stochastic model that allows generating the efficient frontier of final pit limit alternatives under geological uncertainty in the expected profit vs. risk context. The variability of the deposit is modelled using several conditional simulations, and the risk of losses is measured in terms of conditional value at risk. The proposed methodology's main advantage is the generation of an optimal policy to manage the trade-off between expected profit and risk, represented by the efficient frontier, allowing the evaluator to make the best decision according to the mining company's interests and its aversion to risk.

To test the performance of the proposed methodology to determine final pits, the efficient frontier obtained was compared with different approaches available in the literature. The criterion used was to minimize the distance to the ideal point (DIP, the unfeasible final pit with maximum expected profit and minimum risk along the efficient frontier). Our approach shows better results in controlling the risk of suffering economic losses without renouncing high expected profit.

Future research work includes developing new efficient algorithms for finding optimal solutions, because computing time will be a limitation when finding solutions of (P_μ) for a model including millions of blocks and hundreds of conditional simulations representing the geological uncertainty. As an alternative approach, instead of computing the entire efficient frontier of final pits, one may optimize the criterion directly (a priori methods) and compute one optimal solution according to the decision-maker preferences [47,48].

Finally, it would be interesting to explore other criteria to compute optimal solutions or select them from the efficient frontier. This paper proposed some guidelines, and the stochastic dominance ideas developed by [36] are another interesting starting point to continue researching on this topic.

Author Contributions: E.J. and N.M. contributed to the study conception and design, and all authors contributed to the methodology. Material preparation and data collection were performed by E.J. and J.M.O. Analysis were performed by all authors. The first draft of the manuscript was written by E.J. and all authors commented on previous versions of the manuscript. All authors have read and agreed to the published version of the manuscript.

Funding: E. Jélvez was supported by CONICYT/PIA Project AFB180004, and FONDEF/CONICYT IDeA I+D 2019 ID19I10155. J. M. Ortiz was supported by the Natural Sciences and Engineering Council of Canada (NSERC), funding reference number RGPIN2017-04200 and RGPAS-2017-507956. The APC was funded by CONICYT/PIA Project AFB180004.

Institutional Review Board Statement: Not applicable.

Informed Consent Statement: Not applicable.

Data Availability Statement: The data that support the findings of this study are available on reasonable request from the corresponding author. The data are not publicly available due to confidentiality issues.

Acknowledgments: E. Jélvez acknowledges the support of the Chilean National Agency for Research and Development (ANID) PIA-Project AFB180004 and FONDEF/CONICYT IDeA I+D 2019 ID19I10155. J. M. Ortiz acknowledges the support of the Natural Sciences and Engineering Council of Canada (NSERC), funding reference number RGPIN2017-04200 and RGPAS-2017-507956, and of the research sponsors of the Predictive Geometallurgy and Geostatistics Lab at the Robert M. Buchan Department of Mining, Queen's University. They also express their gratitude to Isabel Riveros for her support in the revision of this document.

Conflicts of Interest: The authors declare no conflict of interest.

References

1. Hartman, H. *SME Mining Engineering Handbook*; Volume 2. SME; Britton, S., Gentry, D., Karmis, M., Mutmansky, J., Schlitt, W.Y., Singh, M., Eds.; Society for Mining, Metallurgy and Exploration, Inc.: Littleton, CO, USA, 1992.
2. Chilès, J.-P.; Delfiner, P. *Geostatistics Modeling Spatial Uncertainty*; John Wiley & Sons: New York, NY, USA, 2012.
3. Hustrulid, W.A.; Kuchta, M.; Martin, R.K. *Open Pit Mine Planning and Design, Two Volume Set & CD-ROM Pack*; CRC Press: Boca Raton, FL, USA, 2013; ISBN 978-0-429-17085-0.
4. Lerchs, H.; Grossmann, I.F. Optimum Design of Open-Pit Mines. *Trans. Can. Inst. Min.* **1965**, *58*, 17–24.
5. Hochbaum, D.S. The Pseudoflow Algorithm: A New Algorithm for the Maximum-Flow Problem. *Oper. Res.* **2008**, *56*, 992–1009. [CrossRef]
6. Chandran, B.G.; Hochbaum, D.S. A Computational Study of the Pseudoflow and Push-Relabel Algorithms for the Maximum Flow Problem. *Oper. Res.* **2009**, *57*, 358–376. [CrossRef]
7. Smith, M.; Dimitrakopoulos, R. The Influence of Deposit Uncertainty on Mine Production Scheduling. *Int. J. Surf. Min. Reclam. Environ.* **1999**, *13*, 173–178. [CrossRef]
8. Dowd, P.A. Risk Assessment in Reserve Estimation and Open-Pit Planning. *Trans. Inst. Min. Metall. Sect. A Min. Ind.* **1994**, *103*, A148–A154.
9. Goodfellow, R.; Dimitrakopoulos, R. Simultaneous Stochastic Optimization of Mining Complexes and Mineral Value Chains. *Math. Geosci.* **2017**, *49*, 341–360. [CrossRef]
10. Morales, N.; Seguel, S.; Cáceres, A.; Jélvez, E.; Alarcón, M. Incorporation of Geometallurgical Attributes and Geological Uncertainty into Long-Term Open-Pit Mine Planning. *Minerals* **2019**, *9*, 108. [CrossRef]
11. Mai, N.L.; Topal, E.; Erten, O.; Sommerville, B. A New Risk-Based Optimisation Method for the Iron Ore Production Scheduling Using Stochastic Integer Programming. *Resour. Policy* **2019**, *62*, 571–579. [CrossRef]
12. Maleki, M.; Jélvez, E.; Emery, X.; Morales, N. Stochastic Open-Pit Mine Production Scheduling: A Case Study of an Iron Deposit. *Minerals* **2020**, *10*, 585. [CrossRef]
13. Journel, A.G.; Huijbregts, C. *Mining Geostatistics*; Academic Press: Cambridge, MA, USA, 1978; ISBN 978-0-12-391050-9.
14. Leuangthong, O.; McLennan, J.A.; Deutsch, C.V. Minimum Acceptance Criteria for Geostatistical Realizations. *Nat. Resour. Res.* **2004**, *13*, 131–141. [CrossRef]
15. Emery, X.; Lantuéjoul, C. TBSIM: A Computer Program for Conditional Simulation of Three-Dimensional Gaussian Random Fields via the Turning Bands Method. *Comput. Geosci.* **2006**, *32*, 1615–1628. [CrossRef]
16. Deutsch, C.V.; Journel, A.G. *GSLIB: Geostatistical Software Library and User's Guide*, 2nd ed.; Version 2.0; Oxford University Press: New York, NY, USA, 1998; ISBN 978-0-19-510015-0.
17. Ortiz, J.M. *An Introduction to Sequential Gaussian Simulation*; Annual Report; Predictive Geometallurgy and Geostatistics Lab, Queen's University: Kingston, ON, Canada, 2020; pp. 7–19.
18. Journel, A.G. Geostatistics for Conditional Simulation of Ore Bodies. *Econ. Geol.* **1974**, *69*, 673–687. [CrossRef]
19. Davis, M.W. Production of conditional simulations via the LU triangular decomposition of the covariance matrix. *Math. Geol.* **1987**, *19*, 91–98.
20. Jaime Gómez-Hernández, J.; Mohan Srivastava, R. ISIM3D: An ANSI-C Three-Dimensional Multiple Indicator Conditional Simulation Program. *Comput. Geosci.* **1990**, *16*, 395–440. [CrossRef]
21. Zhang, T.; Switzer, P.; Journel, A. Filter-Based Classification of Training Image Patterns for Spatial Simulation. *Math. Geol.* **2006**, *38*, 63–80. [CrossRef]
22. Mariethoz, G.; Renard, P.; Straubhaar, J. The Direct Sampling Method to Perform Multiple-Point Geostatistical Simulations: Performing Multiple-Points Simulations. *Water Resour. Res.* **2010**, *46*, W11536. [CrossRef]
23. Deutsch, C.V.; Journel, A.G. The Application of Simulated Annealing to Stochastic Reservoir Modeling. *SPE Adv. Technol. Ser.* **1994**, *2*, 222–227. [CrossRef]
24. Oz, B.; Deutsch, C.V.; Tran, T.T.; Xie, Y. DSSIM-HR: A FORTRAN 90 Program for Direct Sequential Simulation with Histogram Reproduction. *Comput. Geosci.* **2003**, *29*, 39–51. [CrossRef]
25. Froidevaux, R. Probability Field Simulation. In *Geostatistics Tróia '92*; Soares, A., Ed.; Quantitative Geology and Geostatistics; Springer: Dordrecht, The Netherlands, 1993; Volume 5, pp. 73–83. ISBN 978-0-7923-2157-6.

26. Whittle, D.; Bozorgebrahimi, A. Hybrid Pits—Linking Conditional Simulation and Lerchs-Grossmann Through Set Theory. In Proceedings of the Symposium on Orebody Modelling and Strategic Mine Planning, Perth, Australia, 22–24 November 2004; pp. 399–404.
27. Alarcón, M.; Emery, X.; Morales, N. Using Simulation to Assess the Trade-off between Value and Reliability in Open Pit Planning. In Proceedings of the 37th International Symposium APCOM 2015, Fairbanks, AK, USA, 31 May 2015; SME: Fairbanks, AK, USA, 2015; pp. 333–342.
28. Maleki, M.; Madani, N.; Jélvez, E. Geostatistical Algorithm Selection for Mineral Resources Assessment and Its Impact on Open-Pit Production Planning Considering Metal Grade Boundary Effect. *Nat. Resour. Res.* **2021**, *30*, 4079–4094. [CrossRef]
29. Dimitrakopoulos, R.; Martinez, L.; Ramazan, S. A Maximum Upside/Minimum Downside Approach to the Traditional Optimization of Open Pit Mine Design. *J. Min. Sci.* **2007**, *43*, 73–82. [CrossRef]
30. Deutsch, M.; Gonzalez, E.; Williams, M. Using simulation to quantify uncertainty in ultimate-pit limits and inform infrastructure placement. *Min. Eng.* **2015**, *67*, 49–55. [CrossRef]
31. Marcotte, D.; Caron, J. Ultimate Open Pit Stochastic Optimization. *Comput. Geosci.* **2013**, *51*, 238–246. [CrossRef]
32. Vielma, J.P.; Espinoza, D.; Moreno, E. Risk Control in Ultimate Pits Using Conditional Simulations. In Proceedings of the 34th APCOM Conference, Vancouver, BC, Canada, 6–9 October 2009; pp. 107–114.
33. Lagos, G.; Espinoza, D.; Moreno, E.; Amaya, J. Robust Planning for an Open-Pit Mining Problem under Ore-Grade Uncertainty. *Electron. Notes Discret. Math.* **2011**, *37*, 15–20. [CrossRef]
34. Espinoza, D.; Lagos, G.; Moreno, E.; Vielma, J. Risk Averse Approaches in Open-Pit Production Planning under Ore Grade Uncertainty: An Ultimate Pit Study. In Proceedings of the 36th APCOM Conference, Porto Alegre, Brazil, 4–8 November 2013; pp. 492–501.
35. Amankwah, H.; Larsson, T.; Textorius, B. Open-Pit Mining with Uncertainty: A Conditional Value-at-Risk Approach. In *Optimization Theory, Decision Making, and Operations Research Applications*; Migdalas, A., Sifaleras, A., Georgiadis, C.K., Papathanasiou, J., Stiakakis, E., Eds.; Springer: New York, NY, USA, 2013; Volume 31, pp. 117–139. ISBN 978-1-4614-5133-4.
36. Acorn, T.; Boisvert, J.B.; Leuangthong, O. Managing Geologic Uncertainty in Pit Shell Optimization Using a Heuristic Algorithm and Stochastic Dominance. *Min. Metall. Explor.* **2020**, *37*, 375–386. [CrossRef]
37. Canessa, G.; Moreno, E.; Pagnoncelli, B.K. The Risk-Averse Ultimate Pit Problem. *Optim. Eng.* **2021**, *22*, 2655–2678. [CrossRef]
38. Sitorus, F.; Cilliers, J.J.; Brito-Parada, P.R. Multi-Criteria Decision Making for the Choice Problem in Mining and Mineral Processing: Applications and Trends. *Expert Syst. Appl.* **2019**, *121*, 393–417. [CrossRef]
39. Hochbaum, D.S.; Chen, A. Performance Analysis and Best Implementations of Old and New Algorithms for the Open-Pit Mining Problem. *Oper. Res.* **2000**, *48*, 894–914. [CrossRef]
40. Artzner, P.; Delbaen, F.; Eber, J.-M.; Heath, D. Coherent Measures of Risk. *Math. Financ.* **1999**, *9*, 203–228. [CrossRef]
41. Rockafellar, R.T.; Uryasev, S. Optimization of Conditional Value-at-Risk. *JOR* **2000**, *2*, 21–41. [CrossRef]
42. Pflug, G.C. Some Remarks on the Value-at-Risk and the Conditional Value-at-Risk. In *Probabilistic Constrained Optimization*; Uryasev, S.P., Ed.; Nonconvex Optimization and Its Applications; Springer: Boston, MA, USA, 2000; Volume 49, pp. 272–281. ISBN 978-1-4419-4840-3.
43. Sarykalin, S.; Serraino, G.; Uryasev, S. Value-at-Risk vs. Conditional Value-at-Risk in Risk Management and Optimization. In *State-of-the-Art Decision-Making Tools in the Information-Intensive Age*; Chen, Z.-L., Raghavan, S., Gray, P., Greenberg, H.J., Eds.; INFORMS: Catonsville, MD, USA, 2008; pp. 270–294. ISBN 978-1-877640-23-0. [CrossRef]
44. Krokhmal, P.; Uryasev, T.; Palmquist, J. Portfolio Optimization with Conditional Value-at-Risk Objective and Constraints. *JOR* **2001**, *4*, 43–68. [CrossRef]
45. Zhu, X.; Li, Y.; Wang, J.; Zheng, T.; Fu, J. Automatic Recommendation of a Distance Measure for Clustering Algorithms. *ACM Trans. Knowl. Discov. Data* **2021**, *15*, 1–22. [CrossRef]
46. Nelis, S.G.; Ortiz, J.M.; Morales, V.N. Antithetic Random Fields Applied to Mine Planning under Uncertainty. *Comput. Geosci.* **2018**, *121*, 23–29. [CrossRef]
47. Lee, J.; Lee, S.-I.; Ahn, J.; Choi, H.-L. Pareto Front Generation with Knee-Point Based Pruning for Mixed Discrete Multi-Objective Optimization. *Struct. Multidiscip. Optim.* **2018**, *58*, 823–830. [CrossRef]
48. Liu, Q.; Li, X.; Liu, H.; Guo, Z. Multi-Objective Metaheuristics for Discrete Optimization Problems: A Review of the State-of-the-Art. *Appl. Soft Comput.* **2020**, *93*, 106382. [CrossRef]